Elucidating the Mode of Action of a Typical Ras State 1(T) Inhibitor

ARTICLE *in* BIOCHEMISTRY · MAY 2014

Impact Factor: 3.02 · DOI: 10.1021/bi401689w · Source: PubMed

7 AUTHORS, INCLUDING:

Daniel Filchinski
Thermo Fisher Scientific
10 PUBLICATIONS **156** CITATIONS
SEE PROFILE

Hans Robert Kalbitzer
Universität Regensburg
301 PUBLICATIONS **5,515** CITATIONS
SEE PROFILE

Michael Spoerner
Universität Regensburg
38 PUBLICATIONS **740** CITATIONS
SEE PROFILE

BIOCHEMISTRY
including biophysical chemistry & molecular biology

Article

pubs.acs.org/biochemistry

Elucidating the Mode of Action of a Typical Ras State 1(T) Inhibitor

Ina C. Rosnizeck,[†] Daniel Filchtinski,[‡] Rui Pedro Lopes,[†] Bärbel Kieninger,[†] Christian Herrmann,[‡] Hans Robert Kalbitzer,[†] and Michael Spoerner*[,†]

[†]University of Regensburg, Institute of Biophysics and Physical Biochemistry, Centre of Magnetic Resonance in Chemistry and Biomedicine, Universitätsstraße 31, 93053 Regensburg, Germany

[‡]Ruhr-University of Bochum, Institute of Physical Chemistry I, Universitätsstraße 150, 44780 Bochum, Germany

ABSTRACT: The small GTPase Ras is an essential component of signal transduction pathways within the cell, controlling proliferation, differentiation, and apoptosis. Only in the GTP-bound form does Ras interact strongly with effector molecules such as Raf-kinase, thus acting as a molecular switch. In the GTP-bound form, Ras exists in a dynamic equilibrium between at least two distinct conformational states, 1(T) and 2(T), offering different functional properties of the protein. Zn^{2+}-cyclen is a typical state 1(T) inhibitor; i.e., it interacts selectively with Ras in conformational state 1(T), a weak effector binding state. Here we report that active *K*-Ras4B, which is prominently found to be mutated in human tumors, exhibits a dynamic equilibrium like *H*-Ras, which can be modulated by Zn^{2+}-cyclen. The titration experiments of Ras with Zn^{2+}-cyclen indicate a cooperatively coupled binding of the ligands to the two interaction sites on Ras that could be identified for *H*-Ras previously. Our data further indicate that as in state 2(T) where induced fit produces the substate 2(T)* after effector binding, a corresponding substate 1(T)* can be detected at the state 1(T) mutant Ras(T35A). The interaction of Zn^{2+}-cyclen with Ras not only shifts the equilibrium toward the weak effector binding state 1(T) but also perturbs the formation of substate 1(T)*, thus enhancing the inhibitory effect. Although Zn^{2+}-cyclen shows an affinity for Ras in only the millimolar range, its potency of inhibition corresponds to a competitive state 2 inhibitor with micromolar binding affinity. Thus, the results demonstrate the mode of action and potency of this class of allosteric Ras inhibitors.

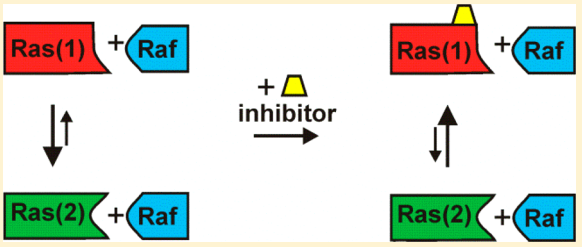

The small guanine nucleotide binding protein (GNB protein) Ras is essentially involved in cellular signal transduction pathways regulating proliferation, differentiation, or apoptosis in mammalian cells. Altering between an inactive, GDP-bound form and an active, GTP-bound form, it acts as a molecular switch. Two classes of regulatory proteins determine the lifetime of these two forms: guanine nucleotide exchange factors (GEFs) and GTPase activating proteins (GAPs). Only in its active form is Ras able to interact properly with effector molecules like Raf-kinase or RalGDS via its switch I region, thus activating the corresponding cellular response (see, e.g., refs 1−3). ^{31}P nuclear magnetic resonance (NMR) spectroscopy, using the bound nucleotide as a probe, reveals a dynamic equilibrium between at least two distinct conformational states in active wild-type Ras and also in its oncogenic variants.[4−7] It could be demonstrated that state 2(T) of Ras is stabilized in its complexes with the Ras binding domains (RBDs) of different Ras effectors such as Raf-kinase, Ral-GDS, AF6, or Byr2.[8−11] Therefore, state 2(T) represents the effector binding state. In accordance with this interpretation, conformational state 1(T) predominates in so-called partial loss-of-function mutants such as Ras(T35S) and Ras(Y40C), thus showing a drastic drop in their affinity for effectors.[6,8,12] Recent results indicate that Ras in state 1(T) is recognized by the catalytic site of the Ras-GEF Sos.[13]

Oncogenic Ras is known to be a key player within the formation of human malignancies because of its lock in the active, GTP-bound form.[14,15] Hence, intensive effort is put into the development of inhibitors of Ras signaling (for reviews see, e.g., refs 1 and 16−20). Besides other targets within the Ras signaling pathways and post-translational processing of Ras, there have been extensive efforts to find small compounds that directly interact with Ras protein with the aim of interrupting Ras-mediated signal transduction (for a review, see ref 21). Currently, there is much effort being spent to inhibit the interaction of Ras with its GEF proteins, thus blocking activation.[22−26] A further strategy is the direct inhibition of Ras−effector interaction by small compounds,[27−29] which is a challenging approach because of the large interaction surface without obvious binding pockets. Very recent approaches make use of an oncogenic *K*-Ras mutation G12C. The thiol group of the cysteine can be directly addressed by compounds that then covalently modify the active site of this Ras mutant but not the wild type. This was used to bind GDP analogues in the active site[30] to switch off the protein. Other compounds bind covalently to this cysteine residue and further occupy a close allosteric binding site, which leads to an increase in GDP affinity with respect to GTP, thus stabilizing the inactive GDP-bound state.[31] In both cases, activation as well as effector

Received: December 20, 2013
Revised: May 21, 2014
Published: May 27, 2014

   dx.doi.org/10.1021/bi401689w | *Biochemistry* 2014, 53, 3867−3878

interaction can be blocked by this method, fixing the protein in an inactive conformation.

Our approach relies on the modulation of the conformational equilibrium in active *H*-Ras, described above, by suitable ligands to impair the Ras−effector interaction.[32] One suitable class of compounds consists of 1,4,7,10-tetraazacyclododecane metal complexes (M^{2+}-cyclens). Two binding sites of Ras for M^{2+}-cyclens could be detected. One-dimensional ^{31}P NMR and two-dimensional $^{1}H-^{15}N$ HSQC NMR spectroscopy revealed that one compound directly binds in the active center of Ras and is coordinated to the γ-phosphate group of the bound nucleotide exclusively to Ras in conformational state 1(T), i.e., the weak binding state for effectors.[33−35] The second binding site is at the C-terminus of the protein and seems to be directly coordinated to the imidazole of His166. Three-dimensional structures of the different M^{2+}-cyclen complexes with Ras have been reported.[35] Similar results were obtained for M^{2+}-(bis-2-picolyl)amine complexes.[36]

In this work, we use ^{31}P NMR spectroscopy, stopped-flow kinetics, and fluorescence titration measurements to gain insight into the mode of perturbation of the Ras effector interaction by a typical state 1(T) inhibitor such as Zn^{2+}-cyclen. We demonstrate that even with this low-affinity binder it is in fact possible to displace Raf-RBD from its high-affinity complex with active Ras in conformational state 2(T) by stabilization of conformational state 1(T). These results indicate that state 1(T) inhibitors should be able to prevent Ras−effector interaction at physiological protein concentrations.

EXPERIMENTAL PROCEDURES

Protein Purification. Wild-type and mutant proteins of the human *K*-Ras4B isoform (amino acids 1−188) and *H*-Ras (amino acids 1−189) were expressed in *Escherichia coli* strain CK600K using ptac expression vectors. Purification was performed using a Q-Sepharose column applying a NaCl gradient followed by size exclusion chromatography of the concentrated Ras-containing fractions.[37] Both Ras isoforms were obtained with a final purity of >95% as judged via sodium dodecyl sulfate−polyacrylamide gel electrophoresis. Nucleotide exchange from GDP to GppNHp of both *K*-Ras and *H*-Ras variants was performed in Mg^{2+}-free buffer with 200 mM $(NH_4)_2SO_4$ using alkaline phosphatase treatment in the presence of a 2-fold excess of the GTP analogue at 5 °C overnight. Free nucleotides, salt, and alkaline phosphatase were removed by size exclusion chromatography. The concentration of active, nucleotide-bound Ras was determined via the nucleotide concentration by C18 reversed phase liquid chromatography using a calibrated detector system (absorbance of guanine at 254 nm). The Ras binding domain of human Raf-1 kinase (Raf-RBD, amino acids 51−131) was expressed in *E. coli* BL21(DE3) using a pGex-2T expression vector. The Raf-RBD-GST fusion protein was cleaved by thrombin on the GSH column overnight at 4 °C. The eluted and concentrated Raf-RBD was further purified by size exclusion chromatography.[38]

Labeling with IAEDANS. Purified *H*-Ras(1−166) Y32C/C118S (150 μM) bound to GppNHp in 50 mM Tris-HCl (pH 7.4), 100 mM NaCl, 5 mM $MgCl_2$, and 3 mM ascorbic acid were mixed with a 5-fold molar excess of IAEDANS (stock dissolved in dimethylformamide). After an overnight incubation at 4 °C, the coupling reaction was stopped by addition of a 10-fold molar excess of DTT, and the excess of IAEDANS was removed by gel filtration using Zeba Spin Desalting Columns (Pierce) equilibrated with the buffer containing 15 mM Hepes-NaOH (pH 7.4), 125 mM NaCl, and 5 mM $MgCl_2$.

NMR Spectroscopy. The Ras·Mg^{2+}·nucleotide complex (1−1.5 mM) was dissolved in buffer A [40 mM Tris-HCl (pH 7.5), 10 mM $MgCl_2$, 2 mM DTE, and 0.1 mM DSS (sodium 4,4-dimethyl-4-silapentane-1-sulfonate) containing a 5% D_2O/95% H_2O mixture]. For measurements performed in the presence of Raf-RBD, 150 mM NaCl was added to avoid protein dimerization. The ^{31}P NMR spectra were recorded with a Bruker Avance-500 NMR spectrometer operating at a ^{31}P frequency of 202 MHz using a 70° pulse and a repetition time of 7 s. Measurements were performed in a ^{31}P selective 10 mm probe using 8 or 10 mm Shigemi sample tubes at various temperatures. Protons were decoupled during data acquisition by a GARP sequence[39] with a strength of the B_1 field of 830 Hz. For each ^{31}P NMR spectrum, a ^{1}H NMR spectrum was recorded. For the referencing of the ^{31}P NMR spectra, a Ξ value of 0.4048073561 reported by Maurer and Kalbitzer[40] was used, which corresponds to 85% external phosphoric acid contained in a spherical bulb. The temperature was controlled by determining the line separation (methyl hydrogens-hydroxyl) of external methanol for calibration.[41] All spectra were recorded at a temperature of 278 K. The absolute accuracy of the temperatures given here is better than ±0.5 K. Experimental data have been filtered exponentially, leading to an additional line broadening of 15 Hz.

Binding of Zn^{2+}-cyclen to *K*-Ras and *H*-Ras in state 1(T) follows the fast exchange condition on the NMR time scale; therefore, the change in the chemical shift of the phosphate groups is proportional to the fraction of the Zn^{2+}-cyclen bound form of Ras in the state 1(T) conformation. The ligand concentration at half-saturation that corresponds to the microscopic dissociation constant K_D as well as a coefficient of cooperativity n can be determined by the Hill equation:[42,43]

$$\delta - \delta_f = (\delta_c - \delta_f)\frac{[L]_f^{\,n}}{K_D^{\,n} + [L]_f^{\,n}} = (\delta_c - \delta_f)\frac{\left([L]_0 - N[\mathrm{Ras}]_0\frac{\delta - \delta_f}{\delta_c - \delta_f}\right)^n}{K_D^{\,n} + \left([L]_0 - N[\mathrm{Ras}]_0\frac{\delta - \delta_f}{\delta_c - \delta_f}\right)^n} \quad (1)$$

where δ_f and δ_c are the chemical shift values of free Ras in state 1(T) and in complex with a ligand, respectively. $[\mathrm{Ras}]_0$ and $[L]_0$ are the total concentrations of the protein and the ligand in solution, respectively. $[L]_f$ is the concentration of free ligand. n is the Hill coefficient reflecting the strength of the cooperativity of binding.

Kinetic Measurements. The fluorescence measurement of the binding kinetics was performed with an SFM400 stopped-flow apparatus (BioLogic, Grenoble, France) by rapid mixing of 0.5 μM Ras bound to the GTP analogue GppNHp containing the fluorescent 2′-/3′-*O*-(*N*′-methylanthraniloyl) group (termed mGppNHp) with various concentrations of Raf-RBD in the presence or absence of Zn^{2+}-cyclen. The excitation wavelength was adjusted to 355 nm. The emission was detected using a cutoff filter of 420 nm. The observed rate constants k_{obs} were obtained by fitting a single-exponential function to the time-dependent fluorescence traces. To determine the kinetic parameters, the k_{obs} values were plotted versus the Raf-RBD concentration. A hyperbolic function was fit to the data in the case of the association kinetics measured in the absence of Zn^{2+}-cyclen according to Sydor et al.[44] A linear fit was applied

for the plots of k_{obs} versus the Raf-RBD concentration in the presence of 20 mM Zn^{2+}-cyclen.

Ras·Raf-RBD association kinetics at various concentrations of Zn^{2+}-cyclen and a fixed concentration of Raf-RBD were measured by mixing 0.5 μM Ras mGppNHp with 20 μM Raf-RBD; both protein solutions were preincubated with Zn^{2+}-cyclen at various concentrations. The change in fluorescence was recorded, and k_{obs} values were obtained by fitting the fluorescence change by a single-exponential function. The measurements were performed at 10 °C using a buffer containing 15 mM Hepes-NaOH (pH 7.4), 125 mM NaCl, and 5 mM $MgCl_2$.

Fluorescence Titration. The fluorescence titrations were performed in a Kontron (Leipzig) apparatus with 10 nm excitation and emission slits and excitation and emission wavelengths of 340 and 460 nm, respectively. IAEDANS attached to Ras at position 32 was used as a fluorescent probe at concentration of 0.2 μM in the presence or absence of 0.5 μM Raf-RBD. Zn^{2+}-cyclen was added stepwise to the solution, and the change in fluorescence was detected. All fluorescence titration measurements were performed at 298 K in a buffer containing 15 mM Hepes-NaOH (pH 7.4), 125 mM NaCl, and 5 mM $MgCl_2$.

Calculation of the Interaction Sphere in the Rap1A-(E30D,K31E)·Raf-RBD Complex. Protons were added within the X-ray crystal structure of the Rap1A(E30D,K31E)·Raf-RBD complex [Protein Data Bank (PDB) entry 1gua].[45] The residues involved in the protein−protein interactions were defined by two criteria. (i) The water accessible surface of the residue in question decreased in the complex by more than 5%, and (ii) at least one atom of the residue was <0.5 nm from an atom of the interacting protein in the complex. Both criteria were analyzed using the corresponding features of MOLMOL.

RESULTS AND DISCUSSION

Comparison of Conformational Equilibria in *H*-Ras and *K*-Ras4B. The intention of this study is to improve our understanding of the modulation of Ras-mediated signal transduction by addressing the intrinsic conformational equilibria of Ras protein with small molecules. Because the *K*-Ras isoform is found to be most prominently mutated in human cancer, we first investigated *K*-Ras4B in terms of the equilibrium between main conformational states 1(T) and 2(T) that have been extensively investigated for *H*-Ras in previous work. $^{1}H-^{15}N$ HSQC data can basically provide much more detailed structural and dynamical information, but unfortunately in Ras proteins, almost all resonances that correspond to the amino acids located in switch regions are invisible because of the conformational exchange processes. In contrast, ^{31}P NMR spectroscopy allows us to investigate these equilibria in rather simple spectra with a suitable dispersion of the resonance signals. Figure 1A shows the ^{31}P NMR spectra of the full length wild-type proteins of human *H*-Ras(1−189) and *K*-Ras4B(1−188) bound to Mg^{2+}·GppNHp. The obtained spectra look very similar. The corresponding chemical shift values are summarized in Table 1. The γ-phosphate signals representing state 2(T) and state 1(T) are best separated. The integral of each resonance signal reflects directly the population of the corresponding conformational state. One obtains an equilibrium constant for *K*-Ras4B with K_{12} = [state 2]/[state 1] = 2.0, which agrees within error with the value obtained for *H*-Ras (K_{12} = 1.9). An error of ±0.2 has to be considered on the basis of the fitting procedure of the partially superimposed signals

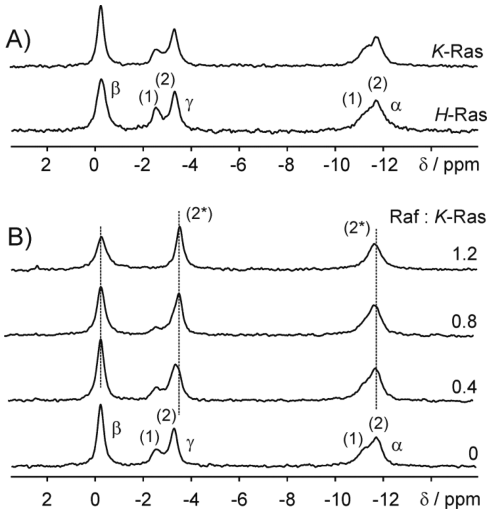

Figure 1. Conformational equilibria in Ras detected by ^{31}P NMR spectroscopy. ^{31}P NMR spectra of complexes of human Ras with Mg^{2+}·GppNHp at 278 K. (A) Wild-type *H*-Ras(1−189) and wild-type *K*-Ras4B(1−188), the resonances corresponding to the α-, β-, and γ-phosphates, and the assignment to state 1(T) and state 2(T) are indicated. The obtained chemical shift values as well as the equilibrium constants are summarized in Table 1. (B) Formation of the complex between *K*-Ras4B and Raf-RBD detected by ^{31}P NMR spectroscopy. To initially 1.3 mM *K*-Ras4B(wt) were added increasing amounts of highly concentrated Raf-RBD. The molar ratio of Raf-RBD to Ras is indicated. The final concentration of *K*-Ras was 0.93 mM.

with the Lorentzian function. The line widths of the γ-phosphate signals indicate similar rates of exchange between the two states in the range of 120 s^{-1} as determined for *H*-Ras(wt) at 278 K.[5] Figure 1B presents the obtained ^{31}P NMR spectra on the titration of *K*-Ras4B(wt) with the Ras binding domain (RBD) of the effector Raf-kinase. The effects can be detected very clearly: with increasing amounts of effector RBD, new resonance lines with chemical shifts close the values corresponding to state 2(T) arise. At the same time, the integrals of the resonances that correspond to Ras in state 1(T) decrease and disappear at equimolar concentrations of the effector. The same observations were published previously for wild-type *H*-Ras.[4,5,12]

Modulation of the Conformational Equilibrium in *K*-Ras by a State 1(T) Inhibitor. To verify if the conformational equilibrium detected in *K*-Ras4B can also be addressed by Zn^{2+}-cyclen treatment as *H*-Ras, we titrated the wild-type proteins of both isoforms in complex with Mg^{2+}·GppNHp with Zn^{2+}-cyclen under identical conditions (Figure 2A,C). As published previously for *H*-Ras[33] in both Ras isoforms, the magnitudes of signals corresponding to state 2(T) decrease with higher concentrations of the ligand whereas the magnitudes of signals corresponding to state 1(T) increase simultaneously showing downfield shifts of the α- and γ-phosphate signals and an upfield shift of the β-phosphate signal (Figure 2A). The interaction of the ligand with Ras in state 1(T) follows the fast exchange condition of the γ-phosphate signal on the NMR time scale; i.e., one obtains one shifting resonance signal with increasing concentrations of the ligand. From this behavior, we can estimate that the off rate between Zn^{2+}-cyclen and both Ras isoforms in state 1(T) has to be much higher than the determined line separation ($\Delta\nu$) of the free and Zn^{2+}-cyclen-bound states; i.e., $k_{off} \gg 200$ s^{-1}. In Figure 2B, the chemical shift change of the γ-phosphorus resonance in state 1(T)

dx.doi.org/10.1021/bi401689w | *Biochemistry* 2014, 53, 3867−3878

Table 1. ^{31}P NMR Chemical Shift Values of *H*-Ras and *K*-Ras4B·Mg^{2+}·GppNHp Complexes[a]

	α-phosphate		β-phosphate		γ-phosphate		
Mg^{2+} ·GppNHp	δ_1 (ppm)	δ_2 (ppm)	δ_1 (ppm)	δ_2 (ppm)	δ_1 (ppm)	δ_2 (ppm)	K_{12}[b]
K-Ras4B(wt) (1−188)	−11.27	−11.73	−0.32	−0.21	−2.58	−3.30	2.0
with Raf-RBD		−11.62		−0.26		−3.52	
H-Ras(wt) (1−189)[c]	−11.25	−11.71	−0.26	−0.16	−2.54	−3.24	1.9
with Raf-RBD		−11.65		−0.19		−3.57	
H-Ras(T35S) (1−189)[c]	−11.10		−0.32		−2.57		<0.1
with Raf-RBD		−11.60		−0.29		−3.41	
H-Ras(T35A) (1−189)[c]	−11.09		−0.33		−2.49		<0.1
with Raf-RBD	−10.78[d]		−0.35[d]		−2.79[d]		
H-Ras(G12V) (1−189)[c]	−11.24	−11.55		−0.25[e]	−2.36	−4.08	0.9
with Raf-RBD		−11.60		−0.23		−4.46	
H-Ras(G13R) (1−189)	−11.11	11.45	0.45	0.15	−1.79	−4.43	2.5
with Raf-RBD		−11.42		−0.23		−4.48	
H-Ras(Q61A) (1−189)	−11.13	−11.62		−0.21[e]	−2.47	−3.41	2.6
with Raf-RBD		−11.62		−0.27		−3.66	

[a]All values are determined from spectra recorded at 278 K and pH 7.5 in the presence of 10 mM $MgCl_2$. The estimated error from the fitting procedure is less than ±0.05 ppm in chemical shift values. [b]The equilibrium constant is defined as K_{12} = [state 2]/[state 1], derived from the integrals of the corresponding NMR signals. The error form the fitting procedure is ±0.1. For the wild-type proteins, it is ±0.2 because of the superposition of the γ-phosphate lines. [c]Please note that comparable published data are available. See refs 5, 8, and 12. [d]The errors in chemical shift are ±0.1 because of the superposition of the signals. [e]Resonance signals are not separated.

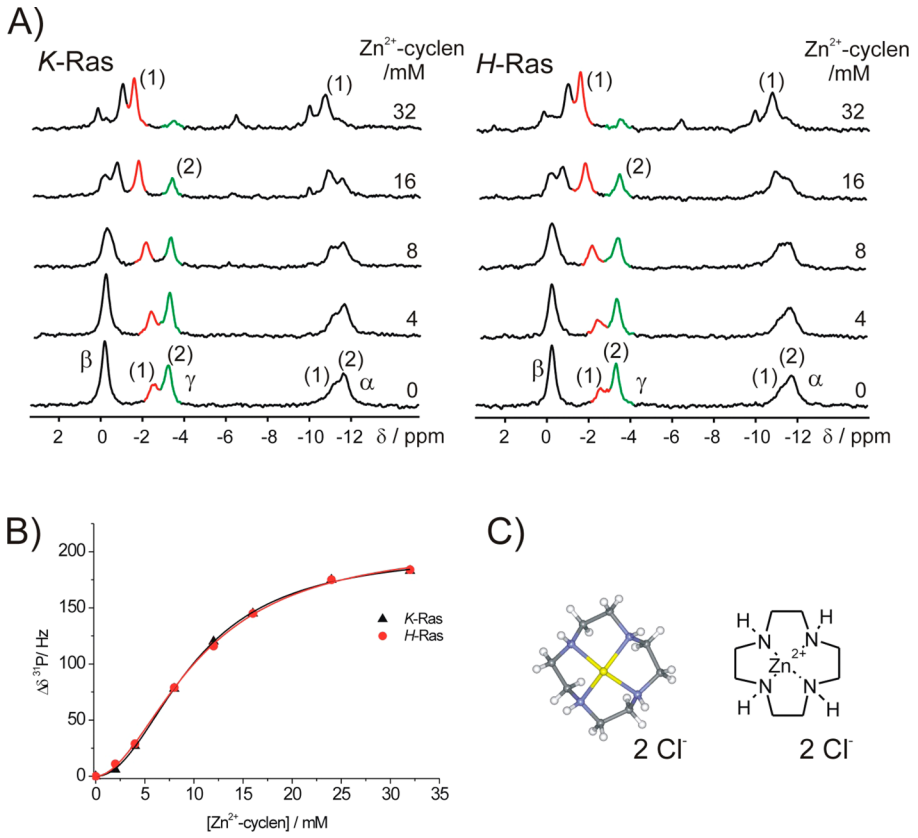

Figure 2. ^{31}P NMR spectroscopy on the titration of wild-type Ras·Mg^{2+}·GppNHp complexes with Zn^{2+}-cyclen. (A) ^{31}P NMR spectra of initially 1.3 mM *K*-Ras4B(wt) (left) and 1.3 mM *H*-Ras(wt) (right) in the presence of increasing concentrations of Zn^{2+}-cyclen at 278 K. The concentrations of Zn^{2+}-cyclen are indicated. In the final spectra at high concentrations of the ligand, additional small signals become visible at chemical shifts of 0.3, −6.5, and −10.0 ppm that correspond to the γ-, β-, and α-phosphates, respectively, of free Mg^{2+}·GppNHp. (B) Plot of the obtained chemical shift changes of the γ-phosphate resonance in state 1(T) induced by Zn^{2+}-cyclen (see spectra presented in panel A) as a function of ligand concentration. The obviously sigmoidal curve progressions were fit by the Hill equation (eq 1 in Experimental Procedures). The obtained $\Delta\delta_{max}$ value for *K*-Ras is 200 ± 3 Hz; the obtained microscopic dissociation constant (K_D) is 9.9 ± 0.2 mM, and the Hill coefficient (n) is 2.0 ± 0.1. The corresponding values obtained for *H*-Ras are 200 ± 3 Hz, 10.4 ± 0.3 mM, and 1.9 ± 0.1, respectively. (C) Structure of the 1,4,7,10-tetraazacyclododecane·Zn^{2+} complex, in which Cl^- ions served as counterions.

dx.doi.org/10.1021/bi401689w | *Biochemistry* 2014, 53, 3867−3878

induced by Zn^{2+}-cyclen interaction is plotted as a function of ligand concentration. For both Ras isoforms, very similar results are obtained. The plotted values describe a sigmoidal progression. The data of both Ras isoforms can be fit by the Hill equation assuming two binding sites (see Experimental Procedures) leading to Hill coefficients of 1.9 ± 0.1 and 2.0 ± 0.1 for *H*-Ras and *K*-Ras, respectively. Experimentally, two Zn^{2+}-cyclen binding sites were identified for *H*-Ras. A Hill coefficient close to the number of binding sites is characteristic of a large positive cooperativity. The obtained microscopic dissociation constants are 10.4 ± 0.3 and 9.9 ± 0.2 mM for *H*-Ras and *K*-Ras4B, respectively (see Experimental Procedures). The *K*-Ras4B isoform as *H*-Ras provides a histidine residue in position 166 that was shown to be involved in the ligand interaction at that second binding site on *H*-Ras.[35] This result also shows that *K*-Ras4B can be targeted by state 1(T) inhibitors and shows features very similar to those of *H*-Ras.

In the spectra shown in Figure 2A, additional small signals become visible at chemical shifts of 0.3, −6.5, and −10.0 ppm that correspond to the γ-, β-, and α-phosphates, respectively, of free Mg^{2+}·GppNHp. The free nucleotide is observed at higher M^{2+}-cyclen concentrations. This seems to be the result of a lower affinity between the nucleotide and Ras. Indeed, the presence of Zn^{2+}-cyclen increases slightly the k_{off} (a factor of 3 was observed in the presence of 20 mM Zn^{2+}-cyclen). In the equilibrium (there was no additional nucleotide added to the buffer), this could result in a small fraction of nucleotide-free Ras that is less stable and thus tends to aggregate and precipitate. During the rather time-consuming ^{31}P NMR experiments (several hours per titration step), a small amount of protein precipitated.

In summary, the findings obtained here and in previous investigations of *H*-Ras variants are expected to be able to be transferred to *K*-Ras4B to a large extent. As in the wild type, also in oncogenic variants of *H*-Ras the 1(T)−2(T) equilibrium is detected by ^{31}P NMR spectroscopy.[5,8] The chemical shift values and equilibrium constants of some oncogenic Ras variants containing a mutation in the common amino acid position 12, 13, or 61 are listed in Table 1. It could be shown that conformational state 1(T) can also be addressed in oncogenic variants by a state 1(T) inhibitor such as Zn^{2+}-cyclen or Zn^{2+}-BPA.[36]

Kinetics of Association and Dissociation of Raf-RBD with *H*-Ras·mGppNHp in the Presence of Zn^{2+}-Cyclen. To characterize the inhibitory effect of Zn^{2+}-cyclen on the Ras−Raf interactions, the association and dissociation kinetics were recorded in the presence of Zn^{2+}-cyclen. The kinetics are studied with Ras in complex with a GTP analogue containing a fluorescent 2′-/3′-*O*-(*N*′-methylanthraniloyl) group (termed mGppNHp throughout).[12,44] In fact using mGppNHp in complex with *H*-Ras has only a small effect on the conformational equilibrium as deduced from the corresponding ^{31}P NMR spectra.[8] In the presence of 25 mM Zn^{2+}-cyclen, the observed association rate constant displays a linear dependence on Raf-RBD concentration that is in contrast to the hyperbolic dependence of the observed rate constant of the Ras−Raf interaction in the absence of Zn^{2+}-cyclen (Figure 3A) in the same concentration range of Raf-RBD.[12,44] Using a linear fit, an apparent association rate constant (k'_{on}) of 2.2 μM^{-1} s^{-1} could be determined. This apparent association rate constant is by 1 order of magnitude smaller than the association rate constant determined for the Ras−Raf association kinetics in the absence of Zn^{2+}-cyclen obtained from the hyperbolic fit as a consequence of a two-state association model yielding a k_{on} of 19.0 μM^{-1} s^{-1}. A similar linear dependence of the association rate constant on the Raf-RBD concentration was observed earlier for the state 1(T) mutant Ras(T35A);[12] i.e., a similar decrease in k_{on} to 0.7 μM^{-1} s^{-1} was observed, without showing any indication of saturation of the plotted k_{obs} values within the Raf concentration range used in the experiments. These results

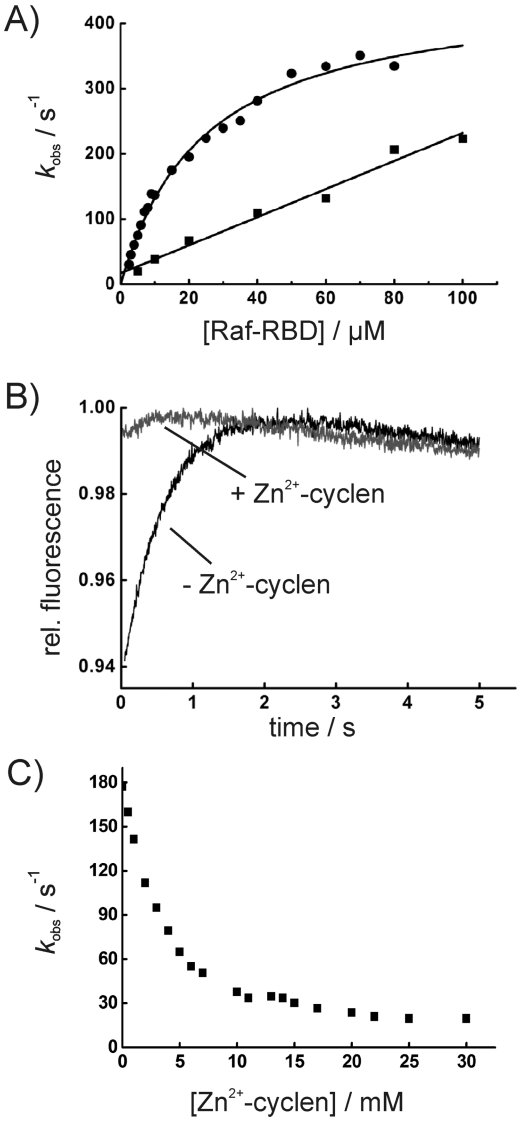

Figure 3. Effect of Zn^{2+}-cyclen on the kinetics of association between *H*-Ras(1−189) and Raf-RBD. All measurements were performed at 283 K. (A) Stopped-flow kinetics of the association between Raf-RBD and *H*-Ras(wt)·Mg^{2+}·mGppNHp in the absence (●) and presence (■) of 25 mM Zn^{2+}-cyclen. The obtained k_{obs} values for the binding of Raf-RBD to Ras are plotted vs Raf-RBD concentration. A hyperbolic or linear function was applied to the data according to refs 12 and 44. (B) Stopped-flow dissociation kinetics performed on the complex between *H*-Ras(wt)·Mg^{2+}·mGppNHp (0.5 μM) and Raf-RBD (10 μM). The dissociation of the protein complex was investigated in the absence (black) and presence (gray) of 20 mM Zn^{2+}-cyclen by fast mixing with nonfluorescent *H*-Ras-GppNHp (200 μM). (C) Stopped-flow association kinetics between *H*-Ras(wt)·Mg^{2+}·mGppNHp (0.5 μM) in the presence of increasing concentrations of Zn^{2+}-cyclen and 20 μM Raf-RBD. The obtained k_{obs} values are plotted as a function of the Zn^{2+}-cyclen concentration.

dx.doi.org/10.1021/bi401689w | *Biochemistry* 2014, 53, 3867−3878

are to be expected, assuming the stabilization of conformational state 1(T) that led to *H*-Ras(T35A)-like association behavior.[12]

To determine the dissociation rate constant (k_{off}), the preformed *H*-Ras(wt)·mGppNHp·Raf-RBD complex in the absence and presence of Zn^{2+}-cyclen was rapidly mixed with a large molar excess of nonlabeled Ras-GppNHp (Figure 3B). In the absence of Zn^{2+}-cyclen, the dissociation of the *H*-Ras(wt)·mGppNHp·Raf-RBD complex is observed as fluorescence increase and a k_{off} value of 1.6 s^{-1} could be determined by fitting time-dependent fluorescence traces to a single-exponential function.[12] In contrast, only a very small fluorescence increase could be observed in the presence of 20 mM Zn^{2+}-cyclen. This result is not consistent with the k_{off} value of 5.1 s^{-1} obtained for the dissociation of Raf-RBD in complex with state 1(T) mutant Ras(T35A) in previous work.[12] One possible reason could be based on a preformed equilibrium between different complexes. In that case, the small change in fluorescence could be explained by compensating effects caused by the decrease in the fluorescence intensity induced by binding of Zn^{2+}-cyclen to Ras and the obtained increase in the fluorescence intensity as a consequence of dissociation of Raf-RBD from the Ras complex during fast mixing of the preformed equilibrium with nonfluorescent Ras·GppNHp. The inhibitory effect of Zn^{2+}-cyclen on the Ras(wt)−Raf association kinetics was further investigated at various Zn^{2+}-cyclen concentrations. To obtain the observed association rate constants, single-exponential functions were fit to the obtained time-dependent fluorescence traces and the resulting k_{obs} values were plotted as a function of Zn^{2+}-cyclen concentration (Figure 3C). The observed rate constants decreased with increasing Zn^{2+}-cyclen concentration, with k_{obs} values converging to very small values at higher Zn^{2+}-cyclen concentrations.

Effect of Zn^{2+}-Cyclen on Raf-RBD Bound to Ras·Mg^{2+}·GppNHp Studied by ^{31}P NMR Spectroscopy. The fluorescence experiments described above clearly reveal an inhibitory effect of Zn^{2+}-cyclen on the interaction between active Ras and its main downstream target Raf. The detailed mechanism can be further clarified by ^{31}P NMR spectroscopy, using the bound nucleotide as a probe. For the following investigations, we used state 1(T) mutants *H*-Ras(T35S) and *H*-Ras(T35A) that both exist in state 1(T) in the absence of effectors. Whereas the T35S mutant can adopt state 2(T)* in complex with effectors, *H*-Ras(T35A) remains in a state 1(T)-like conformation even in the complex, as deduced from the corresponding ^{31}P NMR chemical shifts.[4,7,8,12]

In contrast to the investigations of wild-type Ras or its oncogenic variants that exist intrinsically in a state 1(T)−2(T) equilibrium with prominent populations of both states, the T35S mutant allows us to discriminate between the effects caused by Zn^{2+}-cyclen interaction and that of effector binding to Ras. Zn^{2+}-cyclen interaction leads to large changes in chemical shifts of the resonances corresponding to conformational state 1(T), whereas the Ras−Raf complex is reflected by the resonance lines with chemical shift values typical for state 2(T)* (Table 1). Therefore, we can directly and quantitatively distinguish between effector-bound and effector-free Ras. Figure 4A shows the ^{31}P NMR data of the *H*-Ras(T35S)·Mg^{2+}·GppNHp complex. The three phosphate groups are represented by one set of signals (Figure 4A, bottom spectrum). Upon addition of a 1.5-fold molar excess of Raf-RBD (i.e., 1.7 mM), *H*-Ras(T35S) is largely saturated with the effector-RBD represented by signals with typical ^{31}P chemical shift values of the complex (Table 1). The resonance signals

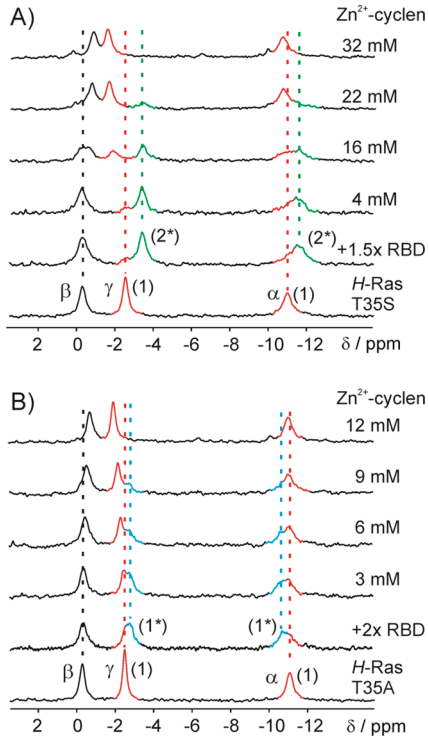

Figure 4. ^{31}P NMR spectroscopy of the displacement of Raf-RBD from *H*-Ras·Mg^{2+} complexes by Zn^{2+}-cyclen. (A) Displacement of Raf-RBD from *H*-Ras(T35S)·GppNHp by Zn^{2+}-cyclen. *H*-Ras(T35S)·GppNHp in the absence (bottom) and presence of a 1.5-fold excess of Raf-RBD (i.e., 1.7 mM) and subsequent addition of a highly concentrated Zn^{2+}-cyclen solution to a final concentration of 32 mM. The respective Zn^{2+}-cyclen concentration is indicated in the spectra. All spectra were recorded at 278 K. The dotted red and green lines indicate chemical shifts corresponding to state 1(T) and the effector-bound state [state 2(T)*], respectively. (B) Displacement of Raf-RBD from *H*-Ras(T35A)·GppNHp by Zn^{2+}-cyclen. This mutant remains in the state 1(T)-like form even in complex with effectors. *H*-Ras(T35A)·GppNHp in the absence (bottom) and presence of a 2-fold excess of Raf-RBD (i.e., 1.6 mM) and subsequent addition of Zn^{2+}-cyclen, which is indicated in the corresponding spectra. All spectra were recorded at 278 K. The dotted red and blue lines indicate the chemical shifts obtained for free and effector-bound Ras in state 1(T)*, respectively.

characteristic of both states are well separated by 0.50 and 0.84 ppm for the α- and γ-phosphorus resonances, respectively. To the present Ras−Raf complex was added the Zn^{2+}-cyclen stepwise up to a final concentration of 32 mM (Figure 4A). The magnitudes of signals representing conformational state 1(T) increase with higher concentrations of Zn^{2+}-cyclen accompanied by an upfield shift of the β-phosphate signal and downfield shifts of the α- and γ-^{31}P resonances, respectively. The shift directions are identical to those found for the signals representing the weak binding state in the titration of the *H*-Ras(wt)·Mg^{2+}·GppNHp complex with Zn^{2+}-cyclen in the absence of Raf-RBD (see Figure 2 and ref 33). The interaction between Zn^{2+}-cyclen and Ras in conformational state 1(T) is represented by a set of shifting resonances for each phosphate at all titrations steps performed, indicating fast exchange conditions on the NMR time scale; i.e., as found for wild-type Ras, the Zn^{2+}-cyclen−state 1(T) interaction shows a k_{off} of $\gg$200 s^{-1}. However, no significant shift changes are observed for the signals representing effector-bound state 2(T)*, which seems to follow still slow exchange on the NMR

dx.doi.org/10.1021/bi401689w | *Biochemistry* 2014, 53, 3867−3878

time scale; i.e., two separated signals for effector-bound state 2(T) and effector-free state 1(T) are observed. The populations of the latter resonances decrease without showing changes in line shape or chemical shift value. At a Zn^{2+}-cyclen concentration of 32 mM, the corresponding signals disappear within the noise level (Figure 4A). As mentioned before, the integrals of the corresponding resonances reflect directly the populations of effector-bound and effector-free fractions of Ras during the titration. Therefore, we can give an estimation of the inhibitory potency of the compound. The analysis of the integrals (Figure 4A) of the γ-phosphate signals yields a Zn^{2+}-cyclen concentration of 18 mM, at which only 50% of Ras remains in complex with the effector (this corresponds to an IC_{50} value). For an estimation, we can use the Cheng–Prussoff equation.[46] Taking into account a K_D value between Ras(T35S) and Raf-RBD of 2 μM[12] and the known concentration of free Raf-RBD in the sample of 1.1 mM, we obtain an inhibitory effect that corresponds to a competitive state 2(T) inhibitor with a binding constant K_i of <50 μM. This observation clearly reveals that the Ras–effector interaction can be perturbed and inhibited by higher concentrations of Zn^{2+}-cyclen interacting with the weak effector binding state 1(T). There is no further line broadening detected at the signals of the Ras fraction, which exists in conformational state 1(T), when Zn^{2+}-cyclen is bound compared to the titration of Ras with Zn^{2+}-cyclen in the absence of Raf-RBD. This strongly indicates that there is no significant interaction between Raf-RBD in the complex formed by Ras in state 1(T) and Zn^{2+}-cyclen.

To confirm the conclusions stated above, a displacement study has also been conducted with mutant *H*-Ras(T35A). Although it is in a low-affinity state of effectors, it can interact weakly with Raf-RBD at the higher concentration (as used in the ^{31}P NMR experiment), but in contrast to Ras(T35S), it cannot isomerize into the high-affinity state to effectors, namely state 2(T)*.[6,12] Using this mutant, the existence of a possible heterotrimeric complex among Ras·GppNHp in state 1(T), Zn^{2+}-cyclen, and Raf-RBD could be detected (Scheme 1). *H*-Ras(T35A)·Mg^{2+}·GppNHp in complex with Raf-RBD was titrated with Zn^{2+}-cyclen to a final concentration of 12 mM (Figure 4B). The initial addition of Raf-RBD to Ras(T35A) led to slightly shifted additional resonance signals corresponding to a nontypical effector-bound conformational state termed state 1(T)* that are not completely separated (Table 1).[12] With increasing amounts of Zn^{2+}-cyclen, two phosphate lines can be separated for each, the α- and γ-phosphate groups. One increases in intensity and area, while the other representing the complex with the effector decreases in intensity and area (Figure 4B). For the increasing magnitude of the signal of the γ-phosphate group, a downfield shift can also be observed. During the whole titration, the α- and γ-phosphorus resonances that correspond to the effector-bound fraction seem to be unchanged. Significant shift changes can be observed only for the set of resonances that can be assigned to the Zn^{2+}-cyclen-bound fraction. At 12 mM Zn^{2+}-cyclen, the resonances of the originally obtained effector-bound fraction disappeared. From theory also, the heterotrimeric complex is to be expected (however, at a very low relative concentration) when Zn^{2+}-cyclen acts as an allosteric inhibitor. In agreement with theory, these data again point out that a heterotrimeric complex is not formed in a larger portion. A distinct set of peaks can be observed for the fractions bound to effector or to Zn^{2+}-cyclen. Even in the weaker complex obtained between Ras(T35A) and Raf-RBD, effector interaction follows slow exchange on the NMR time scale.

Scheme 1. Minimal Scheme for the Interaction among Ras, Raf-RBD, and M^{2+}-Cyclen[a]

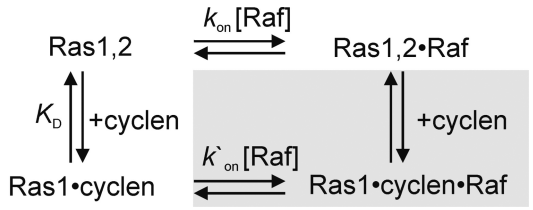

[a]Ras1,2 represents Ras in equilibrium between conformational states 1(T) and 2(T). There is no indication of the binding of M^{2+}-cyclen at the active site of Ras in state 2(T). The gray box shows the complex in question.

Effect of Raf-RBD on the Binding of Zn^{2+}-Cyclen to Ras·Mg^{2+}·GppNHp As Studied by ^{31}P NMR Spectroscopy. From the structural point of view, the displacement of Raf-RBD by Zn^{2+}-cyclen is based on an allosteric mechanism. Because in allosteric regulation, the two binding sites are cooperatively coupled, it should also be possible to release Zn^{2+}-cyclen with higher concentrations of Raf-RBD. Therefore, we performed a further titration starting with the *H*-Ras(wt)·GppNHp·Zn^{2+}-cyclen complex (Figure 5). Upon addition of Zn^{2+}-cyclen, Ras(wt) predominantly existed in conformational state 1(T) with a remaining fraction of Ras in state 2(T) showing a small upfield shift. During the addition of increasing amounts of Raf-RBD to the sample, one observes that the resonances corresponding to Ras in state 1(T) complexed to Zn^{2+}-cyclen decrease, without showing any change in their chemical shift or line width. At the same time, the resonances corresponding to effector-bound state 2(T)* increase. Taking a closer look at the final spectrum, we determined the chemical

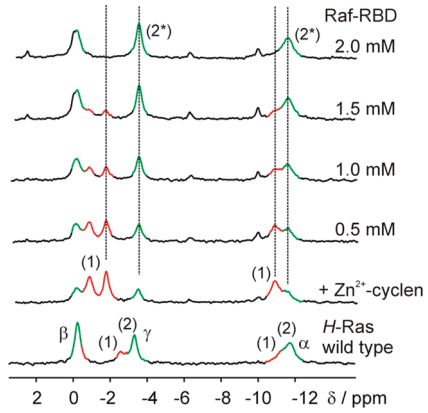

Figure 5. ^{31}P NMR spectroscopy of the titration of the *H*-Ras·Mg^{2+}·GppNHp·Zn^{2+}-cyclen complex with Raf-RBD. To initially 1.3 mM *H*-Ras(wt)·GppNHp was added at first 32 mM Zn^{2+}-cyclen. Into this solution was titrated a highly concentrated Raf-RBD solution to a concentration of 2 mM. The final concentration of Ras was 0.9 mM. The Zn^{2+}-cyclen concentration was kept constant during the whole titration. All experiments were performed at 278 K. The dotted lines indicate the chemical shift corresponding to Ras in effector-bound conformational state 2(T)*. At the high concentration of the ligand, additional small signals become visible at chemical shifts of 0.3, −6.5, and −10.0 ppm that correspond to the γ-, β-, and α-phosphates, respectively, of free Mg^{2+}·GppNHp.

dx.doi.org/10.1021/bi401689w | *Biochemistry* 2014, 53, 3867–3878

shift values to be −11.61, −0.19, and −3.56 ppm for the α-, β-, and γ-phosphates, respectively, typical of those found for the *H*-Ras·Raf complex (Table 1). The chemical shift values of Zn^{2+}-cyclen-bound state 1(T) are unperturbed over the whole concentration range of the titration experiment.

Fluorescence Titration Experiments of Ras·Mg^{2+}·GppNHp with Raf-RBD and Zn^{2+}-Cyclen. To further investigate if the heterotrimeric Ras·Zn^{2+}-cyclen·Raf complex is formed, fluorescence titrations were performed with IAEDANS attached to position 32, which is part of switch I of *H*-Ras (hereafter IS-Ras).[47] Control experiments confirmed that IS-Ras exhibits association kinetics similar to that of wild-type Ras (data not shown).

The IS-Ras·GppNHp complex displays a 2.5-fold fluorescence increase upon binding to Raf-RBD. Zn^{2+}-cyclen was added to the IS-Ras·Raf complex and the fluorescence response detected (Figure 6). The titration of the preformed IS-Ras·GppNHp·Raf-RBD complex with Zn^{2+}-cyclen led to a decrease in fluorescence intensity. Binding of Zn^{2+}-cyclen to IS-Ras also causes an increase in fluorescence intensity indicating a change in the effector binding region upon formation of the IS-Ras·Zn^{2+}-cyclen complex. When the experimental error is taken into account, the fluorescence qualitatively decays upon the titration of the IS-Ras·Raf complex with Zn^{2+}-cyclen to a similar value as it increases upon the titration with Zn^{2+}-cyclen in the absence of the effector. This result further indicates that the formation of the complex between conformational state 1(T) of Ras and Zn^{2+}-cyclen prevents formation of the complex with Raf-RBD and that no trimeric complex is formed at significant concentrations.

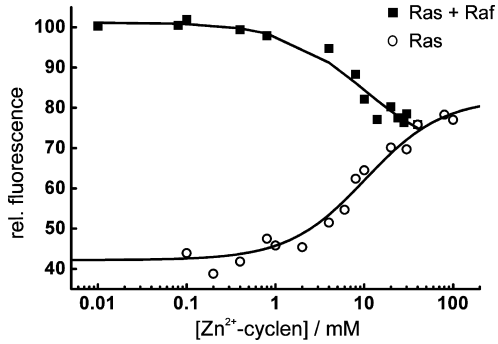

Figure 6. Fluorescence spectroscopy of the titration between Zn^{2+}-cyclen and *H*-Ras or the *H*-Ras·Raf complex. Increasing amounts of Zn^{2+}-cyclen were added to 0.2 μM IS-Ras·Mg^{2+}·GppNHp in the presence (■) or absence (○) of 0.5 μM Raf-RBD. The fluorescence signal obtained from IAEDANS-labeled-Ras was detected as described in Experimental Procedures. The measurements were performed at 298 K. The tendency of the obtained values is given as line for clarity.

Structural Rearrangement of the Effector Interaction Site of Ras by Zn^{2+}-Cyclen. To date, no structure of the complex between Ras and Raf-RBD has been published, but the structure of the complex between the Ras-like Rap mutant Rap1A(E30D,K31E) and Raf-RBD can serve as a model. The calculated interaction sphere between the Rap1A mutant and Raf-RBD (PDB entry 1gua[45]) was derived using the decrease in water accessibility as well as atomic distance restraints (see Experimental Procedures) and plotted on the structure of *H*-Ras(wt)·GppNHp.[48] The residues that are involved in intermolecular polar interactions are labeled in yellow graded color. Residues that are at least partially buried by the effector are labeled in red graded color on the structure of wild-type Ras·GppNHp in Figure 7A. In panels B and C of Figure 7,

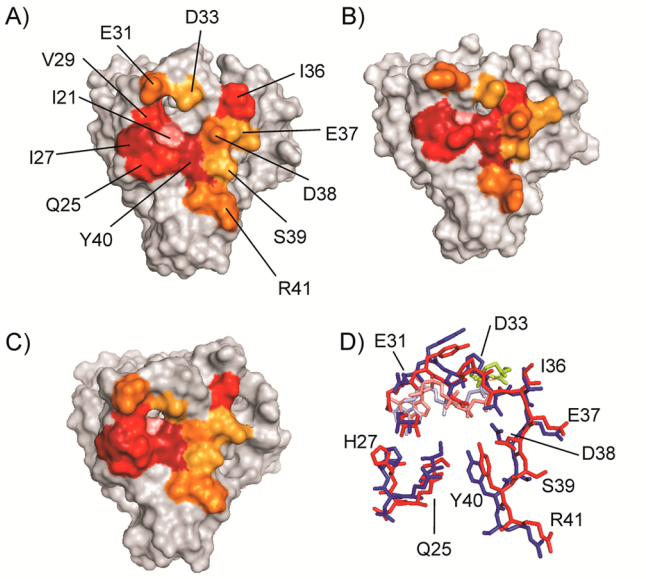

Figure 7. Raf interaction surface plotted on the structures of conformational states 1(T) and 2(T) of *H*-Ras. (A) Raf interaction surface derived from the available complex with Rap1A(E30D,K31E) (PDB entry 1gua)[45] (calculation described in Experimental Procedures) plotted on the structure of *H*-Ras(wt)·GppNHp (PDB entry 5p21):[47] red graded color for residues with decreased solvent accessibility in the complex and yellow graded color for residues involved in polar intermolecular interactions between Rap1A-(E30D,K31E) and Raf-RBD. Note that amino acid types at positions 21, 25, and 27 differ between Rap1A and Ras. (B) Interaction surface derived from the Rap1A(E30D,K31E)·Raf complex plotted on the NMR structure of the state 1(T) mutant *H*-Ras(T35S)·GppNHp (PDB entry 2LCF).[48] (C) Interaction surface derived from the Rap1A(E30D,K31E)·Raf complex plotted on the structure of *H*-Ras(T35A)·GppNHp in complex with Cu^{2+}-cyclen.[35] (D) Superposition of the Raf-interacting residues plotted on the *H*-Ras(T35A)·Cu^{2+}-cyclen complex (red; nucleotides colored light red and cyclen green) and wild-type Ras (blue; nucleotide colored light blue).

these interacting amino acids are plotted in the same color code on the solution structure of Ras(T35S)[48] (Figure 7B) and the NMR-derived calculated structure of Ras(T35A)·GppNHp in complex with M^{2+}-cyclen (Figure 7C).[34] Via comparison of the well-known structure of state 2(T) represented by wild-type Ras, the arrangement of this interaction surface of Ras is disturbed in the complex with M^{2+}-cyclen (Figure 7C). Residues that are disturbed in our calculated structure that initially was derived for the wild-type structure show changes in similar positions as obtained in the solution structure of Ras(T35S). In Ras(T35S), the contact between the Thr35 NH group and the γ-phosphate seems to be interrupted in all structures whereas the contact with Gly60 from switch II could also exist in the conformational ensemble called state 1(T).[49] In the complex structure of Ras with Zn^{2+}-cyclen, both contacts are broken. In Figure 7D, the residues involved in the interaction sphere of wild-type Ras (blue) and Ras(T35A)·M^{2+}-cyclen (red) are shown as a line plot. One can clearly detect distinct conformational changes of residues that are important for direct contacts (polar interactions and hydrogen bonds) within the interaction with Raf, like Glu31, Asp38,

dx.doi.org/10.1021/bi401689w | *Biochemistry* 2014, 53, 3867−3878

Ser39, and Arg41. Furthermore, the surface of the hydrophobic pocket containing Val21, Ile27, and Val29 is structurally reorganized, which should result in steric perturbation of the interaction surface. A reasonable explanation could be that the interaction of Ras in Zn^{2+}-cyclen-bound state 1(T) perturbs the interaction between Gly60 of switch II and the γ-phosphate in addition to the interaction of Thr35 leading to the further decrease in affinity for Raf compared to that of Ras in state 1(T).

CONCLUSIONS AND OUTLOOK

In this work, we demonstrate that full length *K*-Ras4B that is very frequently found to be mutated in solid human tumors[14,15] shows an almost identical behavior in terms of the intrinsic conformational equilibrium that is found for *H*-Ras. Two conformational states dominate in the GppNHp-bound form with an equilibrium constant (K_{12}) of 2. The directed modulation of the conformational equilibrium by stabilizing one conformational state in active *H*-Ras as well as *K*-Ras is a suitable possibility for controlling its signaling activity. Addressing the weak binding state of Ras by small molecules interferes with the effector interaction. It could be shown in former work that *H*-Ras exhibits two binding sites for the small organic compound Zn^{2+}-cyclen. One compound can bind to Ras at the C-terminus with direct interaction with His166 and a further interaction directly at the active center of active Ras in conformational state 1(T) close to the γ-phosphate group.[35] At least the latter mentioned interaction selectively recognizes and stabilizes this weak binding state with effectors at higher concentrations, but the obtained sigmoidal binding curve of the Ras–ligand interaction suggests that Zn^{2+}-cyclen interaction follows strong positive cooperative binding. This is also true for the *K*-Ras4B isoform, which also exhibits the histidine at position 166. The experiments in which the interaction of the Ras effector with Zn^{2+}-cyclen was perturbed using the Ras(T35S) mutant allowed us to distinguish between the Zn^{2+}-cyclen and the effector-bound fraction by ^{31}P NMR spectroscopy. We could demonstrate that although the binding affinity between Zn^{2+}-cyclen and Ras is in the millimolar range, one sees an inhibitory effect comparable to that one would expect for a competitive state 2(T) inhibitor exhibiting a binding affinity in the micromolar range. Because of the allosteric mode of action, the affinity between Ras and the effector is further decreased in the presence of the state 1(T) inhibitor compared to the state 1(T) mutant Ras(T35A). Our data suggest that Zn^{2+}-cyclen binding prevents the major downstream target Raf-RBD from forming a heterotrimeric complex in higher population. As deduced from chemical shift and line width analysis of ^{31}P NMR data as well as fluorescence titration experiments, there was no indication of the formation of a trimeric complex in a significant population detected. This result indicates a further decrease in the affinity of the effector for the Ras·Zn^{2+}-cyclen complex compared to that of Ras in weak effector binding state 1(T).

In light of the new data presented here, we have to modify our established model of Ras conformational states.[33] As shown in the ^{31}P NMR spectrum, the effector binding to Ras leads to a small but significant upfield shift of the γ-phosphate resonance. These experimental data indicated that state 2(T) is modified in the complex with Raf by small conformational changes (usually termed induced fit). Therefore, we already had to introduce conformational state 2(T)* occurring in the complex of wild-type Ras with effectors.[5] Analogously, we find also an upfield shift after binding of Raf to Ras in state 1(T) as demonstrated for the state 1(T) mutant *H*-Ras(T35A). Therefore, the same is true for the weak binding state: ^{31}P NMR data require the introduction of a similar state 1(T)* for the interaction with effectors. In general, it is clear that conformational selection and induced fit are extreme cases, which have to be combined for a detailed description of most real protein–protein interactions. A more complete model is now presented in Figure 8. As a consequence, Zn^{2+}-cyclen not

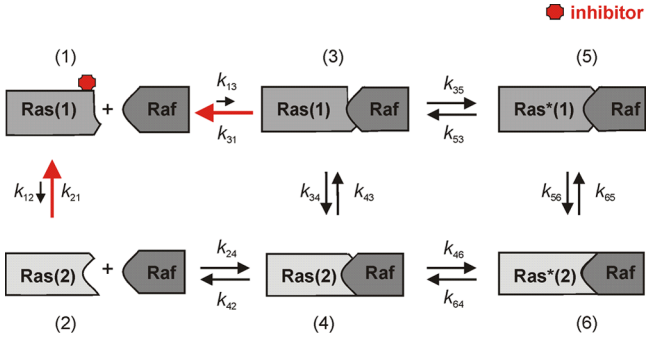

Figure 8. Inhibition mode of state 1(T) inhibitors. The scheme shows the effector interaction of Ras in state 2(T), including the obtained isomerization step into state 2(T)* labeled as Ras*(2). Interaction of the effector with Ras in state 1(T) is obtained in state 1(T) mutant Ras(T35A), which is probably dominated by conformational selection and results in a state 1(T)*, but this mutant cannot isomerize into the state 2(T)* conformation. The state 1(T) inhibitor Zn^{2+}-cyclen perturbs formation of both complexes, resulting in a large decrease in effector affinity.

only stabilizes state 1(T) of Ras, as seen for *H*-Ras(T35A), but also at high concentrations shifts the equilibrium from substate 1(T)* to state 1(T). This means it has a higher affinity for state 1(T) than for state 1(T)*, a property that can be understood qualitatively because effector binding tends to close the nucleotide binding cleft and thus inhibits the binding of the ligand. This property in fact will increase the inhibitory effect of state 1(T) inhibitors. Although the affinity of Zn^{2+}-cyclen for Ras is too low for *in vivo* investigations, our results demonstrate the impact of this type of Ras inhibitor that can be used as a lead compound for the allosteric inhibition of the Ras–effector interaction. A further advantage of cyclen and cyclen derivatives is their direct localization at the active center of Ras close to the common mutations transforming the proto-oncogene Ras.[35] Therefore, it is possible to derive more selective compounds especially for oncogenic Ras variants.

The existence of different conformational states in the thermodynamic equilibrium is of course not restricted to Ras because as a result of fundamental principles the Ras superfamily exhibiting such a regulation cycle should be a common feature of all proteins. To date, the existence of these conformational equilibria has also been reported experimentally by different groups for many other members the Ras superfamily such as Ran, Rho, Cdc42, Rap, Ral, and Arf1.[50−56] Because of the involvement of these compounds in the development of several diseases,[57−63] their interaction with effectors or regulators might also be controlled by the stabilization of a certain conformational state. For the identification of these conformational states, Cu^{2+}-cyclen can be a helpful tool.[64] High-pressure NMR spectroscopy can be used to identify further allosteric binding sites for modulators of

dx.doi.org/10.1021/bi401689w | *Biochemistry* 2014, 53, 3867−3878

Ras signaling.[65] The alteration of these equilibria by selective stabilization of certain states is a promising approach to modulating protein activity in Ras-like proteins.

AUTHOR INFORMATION

Corresponding Author

*University of Regensburg, Institute for Biophysics and Physical Biochemistry, Universitätsstraße 31, 93053 Regensburg, Germany. E-mail: michael1.spoerner@ur.de. Phone: +49 941 943 2495. Fax: +49 941 943 2479.

Author Contributions

I.C.R. and D.F. contributed equally to this work.

Funding

Financial support by the DFG (research training group "Medicinal Chemistry: Molecular Recognition, Ligand-Receptor Interaction"), the DFG Forschergruppe (FOR 1979), and the Volkswagen Foundation is gratefully acknowledged. A grant from Gerhard C. Starck Stiftung to D.F. supported this work. R.P.L. was supported by a grant from the Bayerische Forschungsstiftung.

Notes

The authors declare no competing financial interest.

ACKNOWLEDGMENTS

We thank F. Schmidt and B. König for providing the Zn^{2+}-cyclen.

ABBREVIATIONS

BPA, bis(2-picolyl)amine; cyclen, 1,4,7,10-tetraazacyclododecane; GppNHp, guanosine 5′-(β,γ-imido)triphosphate; IAEDANS, 5-[2-(2-iodoacetamido)ethylamino]naphthalene-1-sulfonic acid; IS-Ras, Ras(Y32C/C118S) residues 1−166 labeled with IAEDANS at position 32; mGppNHp, GppNHp containing the fluorescent 2′-/3′-*O*-(*N*′-methylanthraniloyl) group; RalGDS, guanine nucleotide dissociation stimulator of Ral-GTPase; Ras, gene product of proto-oncogene rat sarcoma; Raf-kinase, rapidly accelerated fibrosarcoma; RBD, Ras binding domain.

REFERENCES

(1) Wittinghofer, A., and Waldmann, H. (2000) Ras: A molecular switch involved in tumor formation. *Angew. Chem., Int. Ed. 39*, 4192−4214.

(2) Herrmann, C. (2003) Ras-effector interactions: After one decade. *Curr. Opin. Struct. Biol. 13*, 122−129.

(3) Rajalingam, K., Schreck, R., Rapp, U. R., and Albert, S. (2007) Ras oncogenes and their downstream targets. *Biochim. Biophys. Acta 1773*, 1177−1195.

(4) Geyer, M., Schweins, T., Herrmann, C., Prisner, T., Wittinghofer, A., and Kalbitzer, H. R. (1996) Conformational transitions in $p21^{ras}$ and its complexes with the effector protein raf-RBD and the GTPase activating protein GAP. *Biochemistry 35*, 10308−10320.

(5) Spoerner, M., Nuehs, A., Ganser, P., Herrmann, C., Wittinghofer, A., and Kalbitzer, H. R. (2005) Conformational states of Ras complexed with the GTP analogue GppNHp or $GppCH_2p$: Implications for the interaction with effector proteins. *Biochemistry 44*, 2225−2236.

(6) Spoerner, M., Nuehs, A., Herrmann, C., Steiner, G., and Kalbitzer, H. R. (2007) Slow conformational dynamics of the guanine nucleotide-binding protein Ras complexed with the GTP analogue GTPγS. *FEBS J. 274*, 1419−1433.

(7) Spoerner, M., Hosza, C., Poetzl, J. A., Reiss, K., Ganser, P., Geyer, M., and Kalbitzer, H. R. (2010) Conformational states of human rat sarcoma (Ras) protein complexed with its natural ligand GTP and their role for effector interaction and GTP hydrolysis. *J. Biol. Chem. 285*, 39768−39778.

(8) Spoerner, M., Wittinghofer, A., and Kalbitzer, H. R. (2004) Perturbation of the conformational equilibria of Ras by selective mutations as studied by ^{31}P NMR spectroscopy. *FEBS Lett. 578*, 305−310.

(9) Geyer, M., Herrmann, C., Wohlgemuth, S., Wittinghofer, A., and Kalbitzer, H. R. (1997) Structure of the Ras-binding domain of RalGEF and implications for Ras binding and signaling. *Nat. Struct. Biol. 4*, 684−699.

(10) Linnemann, T., Geyer, M., Jaitner, B. K., Block, C., Kalbitzer, H. R., Wittinghofer, A., and Herrmann, C. (1999) Thermodynamic and kinetic characterization of the interaction between the Ras binding domain of AF6 and members of the Ras subfamily. *J. Biol. Chem. 274*, 13556−13562.

(11) Gronwald, W., Huber, F., Grünewald, P., Spörner, M., Wohlgemuth, S., Herrmann, C., Wittinghofer, A., and Kalbitzer, H. R. (2001) Solution structure of the Ras binding domain of the protein kinase Byr2 from *Schizosaccharomyces pombe*. *Structure 9*, 1029−1041.

(12) Spoerner, M., Herrmann, C., Vetter, I. R., Kalbitzer, H. R., and Wittinghofer, A. (2001) Dynamic properties of the Ras switch I region and its importance for binding to effectors. *Proc. Natl. Acad. Sci. U.S.A. 98*, 4944−4949.

(13) Kalbitzer, H. R., Spoerner, M., Ganser, P., Hozsa, C., and Kremer, W. (2009) A Fundamental Link between Folding States and Functional States of Proteins. *J. Am. Chem. Soc. 131*, 16714−16719.

(14) Fernández-Medarde, A., and Santos, E. (2011) Ras in Cancer and Developmental Diseases. *Genes Cancer 2*, 344−358.

(15) Karnoub, A. E., and Weinberg, R. A. (2008) Ras oncogenes: Split personalities. *Mol. Cell. Biol. 9*, 517−531.

(16) Gysin, S., Salt, M., Young, A., and McCormick, F. (2011) Therapeutic Strategies for Targeting Ras Proteins. *Genes Cancer 2*, 359−372.

(17) Baines, A. T., Xu, D., and Der, C. J. (2011) Inhibition of Ras for cancer treatment: The search continues. *Future Med. Chem. 3*, 1787−1808.

(18) Friday, B. B., and Adjei, A. A. (2005) K-ras as a target for cancer therapy. *Biochim. Biophys. Acta 1756*, 127−144.

(19) Nussinov, R., Tsai, C. J., and Mattos, C. (2013) 'Pathway drug cocktail': Targeting Ras signaling based on structural pathways. *Trends Mol. Med. 19*, 695−704.

(20) Mattingly, R. R. (2013) Activated Ras as a Therapeutic Target: Constraints on Directly Targeting Ras Isoforms and Wild-Type versus Mutated Proteins. *ISRN Oncol. 2013*, 536529.

(21) Wang, W., Fang, G., and Rudolph, J. (2012) Ras inhibition via direct Ras binding: Is there a path forward? *Bioorg. Med. Chem. Lett. 22*, 5766−5776.

(22) Hocker, H. J., Cho, K. J., Chen, C. Y., Rambahal, N., Sagineedu, S. R., Shaari, K., Stanslas, J., Hancock, J. F., and Gorfe, A. A. (2013) Andrographolide derivatives inhibit guanine nucleotide exchange and abrogate oncogenic Ras function. *Proc. Natl. Acad. Sci. U.S.A. 110*, 10201−10206.

(23) Colombo, S., Palmioli, A., Airoldi, C., Tisi, R., Fantinato, S., Olivieri, S., De Gioia, L., Martegani, E., and Peri, F. (2010) Structure-activity studies on arylamides and arysulfonamides Ras inhibitors. *Curr. Cancer Drug Targets 10*, 192−199.

(24) Maurer, T., Garrenton, L. S., Oh, A., Pitts, K., Anderson, D. J., Skelton, N. J., Fauber, B. P., Pan, B., Malek, S., Stokoe, D., Ludlam, M. J., Bowman, K. K., Wu, J., Giannetti, A. M., Starovasnik, M. A., Mellman, I., Jackson, P. K., Rudolph, J., Wang, W., and Fang, G. (2012) Small-molecule ligands bind to a distinct pocket in Ras and inhibit SOS-mediated nucleotide exchange activity. *Proc. Natl. Acad. Sci. U.S.A. 109*, 5299−5304.

(25) Sun, Q., Burke, J. P., Phan, J., Burns, M. C., Olejniczak, E. T., Waterson, A. G., Lee, T., Rossanese, O. W., and Fesik, S. W. (2012) Discovery of Small Molecules that Bind to K-Ras and Inhibit Sos-Mediated Activation. *Angew. Chem., Int. Ed. 51*, 6140−6143.

(26) Patgiri, A., Yadav, K. K., Arora, P. S., and Bar-Sagi, D. (2011) An orthosteric inhibitor of the Ras-Sos interaction. *Nat. Chem. Biol. 7*, 585−587.
(27) Shima, F., Yoshikawa, Y., Ye, M., Araki, M., Matsumoto, S., Liao, J., Hu, L., Sugimoto, T., Ijiri, Y., Takeda, A., Nishiyama, Y., Sato, C., Muraoka, S., Tamura, A., Osoda, T., Tsuda, K., Miyakawa, T., Fukunishi, H., Shimada, J., Kumasaka, T., Yamamoto, M., and Kataoka, T. (2013) In silico discovery of small-molecule Ras inhibitors that display antitumor activity by blocking the Ras-effector interaction. *Proc. Natl. Acad. Sci. U.S.A. 110*, 8182−8187.
(28) Grant, B. J., Lukman, S., Hocker, H. J., Sayyah, J., Brown, J. H., McCammon, J. A., and Gorfe, A. A. (2011) Novel allosteric sites on Ras for lead generation. *PLoS One 6*, e25711.
(29) Gareiss, P. C., Schneekloth, A. R., Salcius, M. J., Seo, S. Y., and Crews, C. M. (2010) Identification and characterization of a peptidic ligand for Ras. *ChemBioChem 11*, 517−522.
(30) Lim, S. M., Westover, K. D., Ficarro, S. B., Harrison, R. A., Choi, H. G., Pacold, M. E., Carrasco, M., Hunter, J., Kim, N. D., Xie, T., Sim, T., Jänne, P. A., Meyerson, M., Marto, J. A., Engen, J. R., and Gray, N. S. (2014) Therapeutic targeting of oncogenic K-Ras by a covalent catalytic site inhibitor. *Angew. Chem., Int. Ed. 53*, 199−204.
(31) Ostrem, J. M., Peters, U., Sos, M. L., Wells, J. A., and Shokat, K. M. (2013) K-Ras(G12C) inhibitors allosterically control GTP affinity and effector interactions. *Nature 503*, 548−551.
(32) Kalbitzer, H. R., and Koenig, B. (2014) Method and 1,4,7,10-tetraazacyclododecane metal complexes for influencing the spatial structure of Ras or other guanine nucleotide binding (GNB) proteins, and use as antitumor agents. PCT Int. Appl. WO 2004006934 A2 20040122 CAN 140:122769 AN 2004:60322.
(33) Spoerner, M., Graf, T., König, B., and Kalbitzer, H. R. (2005) A novel mechanism for the modulation of the Ras-effector interaction by small molecules. *Biochem. Biophys. Res. Commun. 334*, 709−713.
(34) Schmidt, F., Rosnizeck, I. C., Spoerner, M., Kalbitzer, H. R., and König, B. (2011) Zinc(II)cyclen-Peptide Conjugates Interacting with the Weak Effector Binding State of Ras. *Inorg. Chim. Acta 365*, 38−48.
(35) Rosnizeck, I. C., Graf, T., Spoerner, M., Tränkle, J., Filchtinski, D., Herrmann, C., Gremer, L., Vetter, I. R., Wittinghofer, A., König, B., and Kalbitzer, H. R. (2010) Stabilizing a weak binding state for effectors in the human Ras-protein by small compounds. *Angew. Chem., Int. Ed. 49*, 3830−3833.
(36) Rosnizeck, I. C., Spoerner, M., Harsch, T., Kreitner, S., Filchtinski, D., Herrmann, C., Engel, D., König, B., and Kalbitzer, H. R. (2012) Metal BPA complexes as state 1(T) inhibitors of activated Ras protein. *Angew. Chem., Int. Ed. 51*, 10647−10651.
(37) Tucker, J., Sczakiel, G., Feuerstein, J., John, J., Goody, R. S., and Wittinghofer, A. (1986) Expression of p21 proteins in *Escherichia coli* and stereochemistry of the nucleotide-binding site. *EMBO J. 5*, 1351−1358.
(38) Herrmann, C., Martin, G. A., and Wittinghofer, A. (1995) Quantitative analysis of the complex between p21ras and the Ras-binding domain of the human Raf-1 protein kinase. *J. Biol. Chem. 270*, 2901−2905.
(39) Shaka, A. J., Baker, P. B., and Freeman, R. (1985) Computer-optimized decoupling scheme for wideband applications and low-level operation. *J. Magn. Reson. 64*, 547−552.
(40) Maurer, T., and Kalbitzer, H. R. (1996) Indirect Referencing of ^{31}P and ^{19}F NMR Spectra. *J. Magn. Reson. B113*, 177−178.
(41) Raiford, D. S., Fisk, C. G., and Becker, E. D. (1979) Calibration of methanol and ethylene glycol nuclear magnetic resonance thermometers. *Anal. Chem. 51*, 2050−2051.
(42) Hill, A. V. (1910) The possible effects of the aggregation of the molecules of haemoglobin on its dissociation curves. *J. Physiol. 40*, 4−7.
(43) Goutelle, S., Maurin, M., Rougier, F., Barbaut, X., Bourguignon, L., Ducher, M., and Maire, P. (2008) The Hill equation: A review of its capabilities in pharmacological modelling. *Fundam. Clin. Pharmacol. 22*, 633−648.
(44) Sydor, J. R., Engelhard, M., Wittinghofer, A., Goody, R. S., and Herrmann, C. (1998) Transient kinetic studies on the interaction between Ras and the Ras-binding domain of c-Raf-1 reveal rapid equilibrium of the complex. *Biochemistry 37*, 14292−14299.
(45) Nassar, N., Horn, G., Herrmann, C., Block, C., Janknecht, R., and Wittinghofer, A. (1996) Ras/Rap effector specificity determined by charge reversal. *Nat. Struct. Biol. 3*, 723−729.
(46) Cheng, Y., and Prusoff, W. H. (1973) Relationship between the inhibition constant (K1) and the concentration of inhibitor which causes 50% inhibition (I50) of an enzymatic reaction. *Biochem. Pharmacol. 22*, 3099−3108.
(47) Wohlgemuth, S., Kiel, C., Krämer, A., Serrano, L., Wittinghofer, F., and Herrmann, C. (2005) Recognizing and defining true Ras binding domains I: Biochemical analysis. *J. Mol. Biol. 348*, 741−758.
(48) Pai, E. F., Krengel, U., Petsko, G. A., Goody, R. S., Kabsch, W., and Wittinghofer, A. (1990) Refined crystal structure of the triphosphate conformation of H-*ras* p21 at 1.35 Å resolution: Implications for the mechanism of GTP hydrolysis. *EMBO J. 9*, 2351−2359.
(49) Araki, M., Shima, F., Yoshikawa, Y., Muraoka, S., Ijiri, Y., Nagahara, Y., Shirono, T., Kataoka, T., and Tamura, A. (2011) Solution Structure of the State 1 Conformer of GTP-bound H-Ras Protein and Distinct Dynamic Properties between the State 1 and State 2 Conformers. *J. Biol. Chem. 286*, 39644−39653.
(50) Geyer, M., Assheuer, R., Klebe, C., Kuhlmann, J., Becker, J., Wittinghofer, A., and Kalbitzer, H. R. (1999) Conformational states of the nuclear GTP-binding protein Ran and its complexes with the exchange factor RCC1 and the effector protein RanBP1. *Biochemistry 38*, 11250−11260.
(51) Dias, S. M. G., and Cerione, R. A. (2007) X-ray crystal structures reveal two activated states for RhoC. *Biochemistry 46*, 6547−6558.
(52) Phillips, M. J., Calero, G., Chan, B., Ramachandran, S., and Cerione, R. A. (2008) Effector proteins exert an important influence on the signaling-active state of the small GTPase Cdc42. *J. Biol. Chem. 283*, 14153−14164.
(53) Liao, J., Shima, F., Araki, M., Ye, M., Muraoka, S., Sugimoto, T., Kawamura, M., Yamamoto, N., Tamura, A., and Kataoka, T. (2008) Two conformational states of Ras GTPase exhibit differential GTP-binding kinetics. *Biochem. Biophys. Res. Commun. 369*, 327−332.
(54) Fenwick, R. B., Prasannan, S., Campbell, L. J., Nietlispach, D., Evetts, K. A., Camonis, J., Mott, H. R., and Owen, D. (2009) Solution structure and dynamics of the small GTPase RalB in its active conformation: Significance for effector protein binding. *Biochemistry 48*, 2192−2206.
(55) Fenwick, R. B., Campbell, L. J., Rajasekar, K., Prasannan, S., Nietlispach, D., Camonis, J., Owen, D., and Mott, H. R. (2010) The RalB-RLIP76 complex reveals a novel mode of ral-effector interaction. *Structure 18*, 985−995.
(56) Meierhofer, T., Eberhardt, M., and Spoerner, M. (2011) Conformational states of the ADP ribosylation factor 1 complexed with different guanosine-triphosphates as studied by ^{31}P NMR spectroscopy. *Biochemistry 50*, 6316−6327.
(57) Miertzschke, M., Koerner, C., Spoerner, M., and Wittinghofer, A. (2014) Structural insights into the small G protein Arl13B and implications for Joubert Syndrome. *Biochem. J. 457*, 301−311.
(58) Recchi, C., and Seabra, M. C. (2012) Novel functions for Rab GTPases in multiple aspects of tumour progression. *Biochem. Soc. Trans. 40*, 1398−1403.
(59) Rathinam, R., Berrier, A., and Alahari, S. K. (2011) Role of Rho GTPases and their regulators in cancer progression. *Front. Biosci. 16*, 2561−2571.
(60) Bodemann, B. O., and White, M. A. (2008) Ral GTPases and cancer: Linchpin support of the tumorigenic platform. *Nat. Rev. Cancer 8*, 133−140.
(61) Yuen, H. F., Chan, K. K., Grills, C., Murray, J. T., Platt-Higgins, A., Eldin, O. S., O'Byrne, K., Janne, P., Fennell, D. A., Johnston, P. G., Rudland, P. S., and El-Tanani, M. (2012) Ran is a potential therapeutic target for cancer cells with molecular changes associated with activation of the PI3K/Akt/mTORC1 and Ras/MEK/ERK pathways. *Clin. Cancer Res. 18*, 380−391.

(62) Lewis-Saravalli, S., Campbell, S., and Claing, A. (2013) ARF1 controls Rac1 signaling to regulate migration of MDA-MB-231 invasive breast cancer cells. *Cell. Signalling 25*, 1813−1819.
(63) Donaldson, J. G., and Jackson, C. L. (2011) ARF family G proteins and their regulators: Roles in membrane transport, development and disease. *Nat. Rev. Mol. Cell Biol. 12*, 362−375.
(64) Meierhofer, T., Rosnizeck, I. C., Graf, T., Reiss, K., König, B., Kalbitzer, H. R., and Spoerner, M. (2011) Cu^{2+}-cyclen as probe to identify conformational states in guanine nucleotide binding proteins. *J. Am. Chem. Soc. 133*, 2048−2051.
(65) Kalbitzer, H. R., Rosnizeck, I. C., Munte, C. E., Sunilkumar, P. N., and Spoerner, M. (2013) Intrinsic Allosteric Inhibition of Signaling Proteins by Targeting Rare Interaction States Detected by High Pressure NMR Spectroscopy. *Angew. Chem., Int. Ed. 52*, 14242−14246.